ELSEVIER

Expression profiling using random genomic DNA microarrays identifies differentially expressed genes associated with three major developmental stages of the protozoan parasite *Leishmania major*

Natalia S. Akopyants [a], Robin S. Matlib [a,b], Elena N. Bukanova [a], Matthew R. Smeds [a], Bernard H. Brownstein [a], Gary D. Stormo [b], Stephen M. Beverley [a,*]

[a] *Department of Molecular Microbiology, Center for Infectious Disease Research, Washington University School of Medicine, Campus Box 8230, 660 South Euclid Avenue, Saint Louis, MO 63110, USA*
[b] *Department of Genetics, Washington University School of Medicine, St. Louis, MO 63110, USA*

Abstract

To complete its life cycle, protozoan parasites of the genus *Leishmania* undergo at least three major developmental transitions. However, previous efforts to identify genes showing stage regulated changes in transcript abundance have yielded relatively few. Here we used expression profiling to assess changes in transcript abundance in three stages: replicating promastigotes and infective non-replicating metacyclics, which occur in the sand fly vector, and in the amastigote stage residing with macrophage phagolysosomes in mammals. Microarrays were developed containing 11,484 PCR products that included a number of known genes and 10,464 random 1 kb genomic DNA fragments. Arrays were hybridized in triplicate and genes showing two-fold or greater changes in 2/3 experiments were scored as differentially expressed. Remarkably, only about one percent of the DNAs expression varied by this criteria, in either stage comparison. Northern blot analysis confirmed the predicted change in mRNA abundance for most of these (68%). This set of genes included most of those previously identified in the literature as differentially regulated as well as a number of novel genes. Notably, *Leishmania* maxicircle transcripts showed strong up-regulation in metacyclic and amastigote parasites, probably associated with changes in parasite energy metabolism. However, current data suggest that expression profiling using shotgun DNA libraries significantly underestimates the extent of regulated transcripts.
© 2004 Elsevier B.V. All rights reserved.

Keywords: DNA microarray; *Leishmania*; Genome; Gene expression; Transcriptional regulation; Expression profiling

1. Introduction

Trypanosomatid protozoan parasites of the genus *Leishmania* are the causative agents of leishmaniasis, a widespread group of parasitic diseases varying from spontaneously healing skin lesions to fatal visceral disease. Two million new cases are diagnosed each year with more than 397 million people at risk [1], and in endemic regions leishmaniasis is a common opportunistic AIDS infection [2]. The discovery of visceral leishmaniasis in foxhounds in upper New York State, and the incidence of leishmaniasis in soldiers operating in endemic countries underscore the potential for spread [3,4]. Current hope for new chemother-

apeutic or vaccination therapies lies in research programs oriented towards identifying key processes essential for parasite growth, survival in the mammalian host, or transmission by its insect vector.

Leishmania are transmitted by phlebotomine sand flies to humans and many animal reservoirs. In the sand fly midgut, *Leishmania* replicate as flagellated procyclic promastigotes, which are noninfective. As procyclics enter stationary phase they differentiate to the infective metacyclic stage, which is adapted for transmission to the mammalian host [5]. Once deposited into the host, metacyclics are phagocytosed by macrophages, where they transform into the non-motile, intracellular, replicative amastigote, which are adapted to survive within the hostile environment of the phagolysosome. Understanding how *Leishmania* carry out these developmental transitions and the mechanisms that they employ to survive within each host is critical to the development of

---

effective treatment and cure of these pathogens. The identification of genes whose products show strong stage-specific expression is a well-established paradigm in microbial pathogenesis for the identification of important pathways essential for parasite survival, and one of the goals of the work described here.

Leishmania exhibits an unusual combination of mechanisms of gene expression. Trypanosomatid protozoans use a polycistronic transcriptional approach, in which pre-mRNAs synthesized across hundreds of kb yield monocistronic mRNAs, following processing reactions including a coupling of *trans*-splicing and polyadenylation [6]. Thus, the dependency on promoter-based transcription initiation mechanisms for the control of mRNA level is greatly reduced; perhaps as a result, greater emphasis may be placed on post-transcriptional regulatory mechanisms such as mRNA stability and translation, and protein turnover [7]. Thus far, efforts to identify genes showing stage-dependent variation in transcript abundance, using methods such as subtractive or differential hybridization, or RDA, have yielded only a modest number of regulated genes [8–12]. Nonetheless, many of the genes thus identified have been implicated in key aspects of the parasite infectious cycle.

Many workers have focused on *Leishmania major*, one of the species associated with cutaneous leishmaniasis for which excellent animal models of disease susceptibility and resistance exist [13]. The ∼34 Mb genome of *L. major* is distributed amongst 36 chromosomes and is estimated to encode about 8000 genes [14]. With the eventual availability of the parasite genome and emergence of the field of genome science, new opportunities to probe *Leishmania* gene expression have arisen. Expression profiling through the use of DNA microarrays offers a powerful approach for measuring changes in transcript abundance, as many thousands of genes are studied simultaneously [15,16]. Typically specific probes consisting of either oligonucleotides or DNAs are deposited on solid supports, and hybridization to cDNAs assessed by the aid of fluorophores, which can be either directly or indirectly incorporated into the cDNA.

At the time we initiated these studies a small fraction of the *Leishmania major* genome had been sequenced, and we developed a ∼1-kb random shotgun genomic DNA sequence library and characterized a collection of ∼10,000 of these for use in microarray creation [17]. Similar approaches have been taken with *Plasmodium falciparum* and *Trypanosoma brucei* [18,19]. This tactic seemed well suited for *Leishmania*, as the transcript/gene density is high, introns are exceedingly rare, and the average transcript size is 3.6 kb [17,20,21]. Characterization of this shotgun library set suggested that it was potentially able to identify about 2/3 of all *Leishmania* transcripts [17], making it a useful resource for genome-wide approaches. In this work we have used this DNA collection and expression profiling methodology to focus on the three key parasite stages: replicating promastigotes, infectious metacyclics and amastigotes derived from lesions in mice.

2. Materials and methods

2.1. Parasite culture

Fully virulent *L. major* Friedlin clone V1 (MHOM/JL/80/Friedlin) were grown as promastigotes at 26 °C in one liter bottles containing 500 ml of M199 medium [22] on a rotating platform to increase aeration. Logarithmic growth phase promastigotes were harvested at a density of 2×10^6/ml and were grown in media at pH 7.4. Metacyclic parasites were grown in the same media at pH 5.5 with HEPES replaced 4-morpholinoethanesulfonic acid (MES), and prepared by negative selection with peanut agglutinin (PNA-metacyclics; [5]). Amastigotes were recovered from BALB/cJ mice one month following infection with 5×10^7 stationary phase parasites in the footpad; at this time, the average lesion size was 2–4 mm without visible necrosis [23].

2.2. Nucleic acid isolation and northern blotting

Genomic DNA was isolated from late logarithmic phase promastigotes by the LiCl method [24]. RNA was isolated using the Trizol method (Invitrogen, CA), subsequently treated with DNAse and purified using QIAGEN RNAeasy columns (QIAGEN, Germany). DNA and RNA were quantified by spectrophotometry; RNA was analyzed by Northern blotting as described [25]. The same RNA preparations were used in both microarray and Northern blot experiments. Radiolabeled probes were prepared with the Prime-It II Random Primer Labeling Kit (Stratagene, CA). Hybridization was quantified using a Storm PhosphorImager and IMAGEQUANT software (Amersham Biosciences, CA).

2.3. Shotgun sequence analysis

Sequences from shotgun clones not previously reported were obtained from double-stranded plasmid DNA templates using dye terminators and AmpliTaq DNA polymerase and submitted to the GenBank (NCBI) genome survey sequence (GSS) database (http://www.ncbi.nlm.nih.gov). GenBank accession numbers were CC144545-CC111546 and CC14449-CC144558.

2.4. Microarray preparation

PCR amplified DNAs were generated by using appropriate primers, either gene-specific or the universal M13 forward and M13 reverse primers for the 1 kb random shotgun library; detailed information on the specific DNAs and primers can be obtained from the authors on request. PCR products were purified by ethanol precipitation, washed with 75% ethanol, re-suspended in water, quantified using PicoGreen dye (Molecular Probes, OR) and checked by standard agarose gel electrophoresis. The average DNA concentration was 450 ng μl^{-1}. DNAs were spotted in 0.005% Nonidet P-40 (Sigma, MO) onto poly-L-lysine coated slides

using an Affymetrix 417 arrayer (Affymetrix, CA). cDNA was synthesized from 25 μg of total RNA by direct incorporation of Cy3 or Cy5 fluorophore-labeled dCTP during first-strand synthesis using an oligo (dT) primer (Invitrogen, CA). Three different labeling reactions were done from a single RNA preparation from each stage to facilitate the assessment of technical variability. Hybridizations were performed as described [26] with the following modifications: cDNA was dissolved in 40 μl microarray buffer (Sigma, MO) and hybridization was performed in a water bath at 45 °C for 16 h. The arrays were washed at room temperature in 150 mM NaCl, 15 mM sodium citrate pH 7.5 (1 × SSC) for 5 min and then rinsed twice in 0.2 × SSC for 2 min. Each hybridization experiment was performed in triplicate.

2.5. Data processing and analysis

Hybridization of Cy3- and Cy5-labelled cDNA was quantified using an Affymetrix 428 fluorescent scanner (Affymetrix, CA). From the primary scanned images data were extracted and analyzed using appropriate software (IMAGENE 4.2; BioDiscovery, CA). Depending on the scanner photomultiplier (PMT) setting, the intensity of some spots would fall outside of the linear range of the scanner. Thus each slide was scanned at several PMT settings in order to increase the sensitivity and extend the linear range, and an algorithm was developed to combine these data into a single value.

The data were normalized by setting the median of the $\log_2$ transformed Cy3/Cy5 ratios to zero, for those spots showing intensities at least two-fold over local background, calculated from an annulus around the spot, in both channels. Certain spots that failed this criterion in a single channel were restored to the pool of the candidates after normalization. The complete dataset can be obtained from the authors on request.

3. Results

3.1. Leishmania major microarray creation and RNA recovery across the infectious cycle

DNA microarrays comprising a total of 11,484 DNA elements were created, using PCR-amplified DNAs arising from 10,464 random 1 kb 'shotgun' genomic DNA fragments, 95 ORFs from chromosomes 1 and 3 [21,27], multiple replicas of genes known to be differentially regulated from the literature and our laboratory, and 100 control DNAs (cloning vectors or derived from other species such as mouse, yeast and Escherichia coli). This array of 11,484 elements was used to study differential gene expression for the three major stages of the Leishmania infectious cycle: (1) non-infective replicating procyclic promastigotes, (2) infective, stationary phase metacyclic promastigotes, and (3) amastigotes recovered from a progressing lesion

in BALB/c mice (here the growth phase is undefined and probably heterogeneous).

3.2. Expression profiling of three major Leishmania developmental stages

First, control experiments comparing Cy3- versus Cy5-labeled log phase procyclic promastigote RNA were performed to assess concerns about preferential label incorporation into particular sequences. These data showed that about 0.5% of the spots exhibited two-fold or greater differences in intensity from each other. This 'dye effect' has been seen by others [28] and its basis is not well understood; unless otherwise indicated, we have eliminated these DNAs from the analysis below.

The results from a representative hybridization experiment comparing Cy5-labeled logarithmic phase procyclic RNA versus Cy3-labeled stationary phase metacyclic RNA are summarized in Fig. 1. In this plot we restricted the analysis to the 10,464 random DNA fragments in order to provide an unbiased view of the Leishmania major genome. A plot of the intensities showed that most spots fit a predominantly linear relationship, and that 86% of the spots yielded significant hybridization intensities (two-fold over local background; Fig. 1A). The data in Fig. 1A was first transformed to the $\log_2$ ratio of the Cy5/Cy3 intensities, and then normalized (Fig. 1B; Section 2). Remarkably, most Leishmania spots yielded expression ratios of nearly 1 ($\log_2 = 0$), with only 333 (3.2%) or fewer DNAs in a single experiment showing regulation of greater than two-fold between stages (Fig. 1B). Similar results were obtained in every experiment performed comparing metacyclic or amastigote RNA expression (not shown). In contrast, a similar analysis in the yeast Saccharomyces cerevisiae showed that just the transition from replicating to stationary phase was associated with two-fold or greater changes in expression of 27% of ORF mRNAs (Fig. 1B; [29]).

The data in Fig. 1 and other analyses suggested that expression ratios of less than two-fold potentially could be considered statistically significant. For example, by changing the cut-off to 1.75-fold, the number of spots increased 0.7–1% for any single replicate. However, in keeping with the work of others, the modest number of replicates, and the discussion below, we have focused our discussion to transcripts showing at least two-fold differential expression in the following analysis.

We displayed the results from our studies in the form of Venn diagrams showing the number of DNAs identifying transcripts exhibiting at least two-fold change in one, two or all three experiments for a given developmental transition. In metacyclic versus procyclic promastigotes comparisons (Fig. 2B, Table 1), a total of 333 (3.2%) of the spots showed transcript abundance changes in 1 or more experiments, with 48 (0.5%) in 3/3 experiments and 84 (0.8%) in 2/3 experiments; similar results were obtained with comparisons of amastigotes versus procyclic promastigotes (320,
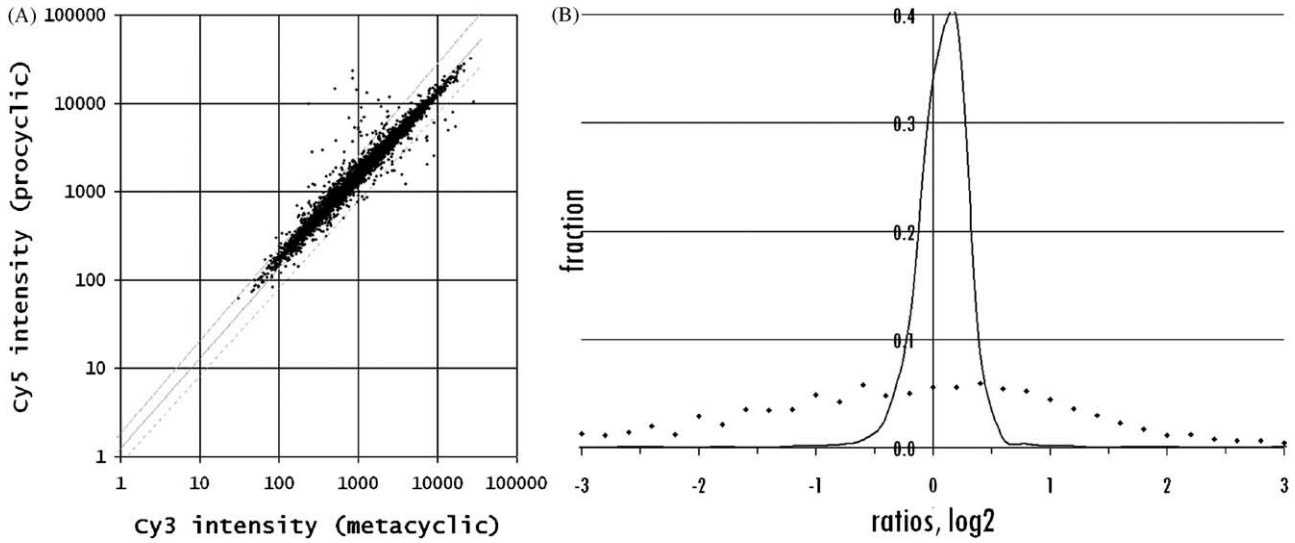
Fig. 1. Expression profiling of procyclic vs. metacyclic transcripts in *L. major*. Panel A: Results of a single representative experiment comparing logarithmic growth phase promastigotes (Cy5, *Y*-axis) vs. PNA- metacyclic parasites (Cy3, *X*-axis). Intensities are shown prior to 'normalization' of Cy3 vs. Cy5 intensities but after adjustment of PMT intensities to account for saturation. The solid line indicates the median after normalization. Dashed lines indicate ±2-fold difference. Panel B: Distribution of log_2 transformed normalized ratios for a single microarray experiment (metacyclic promastigotes versus logarithmic promastigotes; solid black line). A similar analysis of a published data set for logarithmic vs. stationary phase *S. cerevisiae* (dotted line) is shown [29]. Using two-fold or greater changes in relative expression as a criteria, 3.2% of the *L. major* genes varied in this experiment; analogous comparisons yield values of 18–27% in *S. cerevisiae* underoing growth phase transitions or differentiation [29,57].
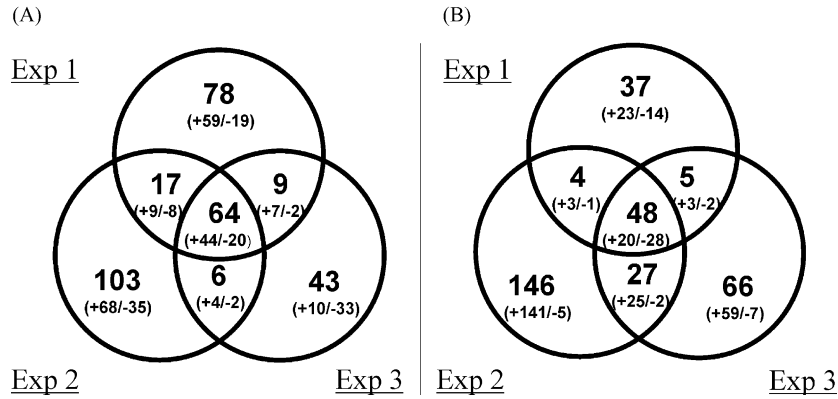

Fig. 2. Venn diagram comparison of microarray datasets for amastigote or metacyclic vs. procyclic promastigote experiments. The results of three different experiments for each comparison are shown in each panel; this analysis includes only the 10,464 random shotgun fragment probes in order to provide an unbiased view of the *Leishmania* genome. The larger number is the total number of spots showing a two-fold or greater change in abundance; "+" or "−", respectively means elevated or decreased relative to logarithmic growth phase procyclic promastigotes: (A) lesion amastigotes; (B) infectious metacyclic promastigotes.

Table 1
Genes showing two-fold or greater changes in transcript abundance by shotgun DNA microarray expression profiling in *Leishmania major*

Experiment	≥1 experiment	≥2 experiments	3 experiments
Lesion amastigotes/logarithmic promastigotes	3.1% (320)	0.9% (96)	0.6% (64)
PNA-metacyclic promastigotes/logarithmic promastigotes	3.2% (333)	0.8% (84)	0.5% (48)

The number in parenthesis refers to the total number of genes identified by each criterion. These data are summarized from Fig. 2 where the breakdown in 'up' or 'down' regulated transcripts abundance is also presented.

64 and 96, respectively; Fig. 2A). Such variation is common in microarray analysis and the results shown in Fig. 2 compare well with similar consistency tests reported by others with different species [30,31].

3.3. Northern blot analysis of DNAs showing differential expression in microarrays

Encouragingly, a survey of the genes scored in the Venn analysis above as 'regulated' in 2/3 experiments or better revealed many that were expected based upon prior studies, including *HASP*, *SHERP*, β-tubulin and histones (discussed below). However, relative transcript levels have been determined for a limited number of *L. major* genes, typically by only a single lab and often for a single developmental transition. Thus we performed Northern blot analysis of procyclic promastigote, metacyclic and amastigote RNAs (the same preparations used in the microarray analysis) for 107 of the shotgun *L. major* fragments. We focused primarily on those genes showing regulation in 2/3 microarray experiments, with a secondary emphasis on those showing regulation in just one or no experiment. Ribosomal RNA staining was used as a control to ensure equal loading amongst samples (Fig. 3F). For most genes (61.7%), one or two mRNA

bands were observed and quantitated; for others (16.7%) a 'smear' was obtained, perhaps indicative of transcripts arising from a multi- or repetitive gene family. Particularly intriguing "smears" arose with probes containing the LTAS telomeric-associated sequences (Fig. 3L). For some genes (21.5%) we did not obtain a Northern blot signal; these were excluded from the statistical analysis below, as the negative result could reflect technical problems and they were not repeated. These data are summarized in Table 2 and representative Northern blots are shown in Fig. 3, including the quantitation derived from the average of the three microarray comparisons for each set of experiments. Examples are shown where the Northern blot and microarray results were in good agreement, as well as ones where discrepancies were found.

First, we considered those comparisons in which expression profiling had predicted at least a two-fold change in expression, for either metacyclic or amastigote versus procyclic comparisons (Table 2). For metacyclic versus logarithmic promastigote comparisons, 27/36 (75%) of the regulated genes identified in our microarray analysis were confirmed, showing at least two-fold changes in expression in Northern blots. For the amastigote versus logarithmic promastigote comparisons, 21/35 (60%) were confirmed by this criterion.
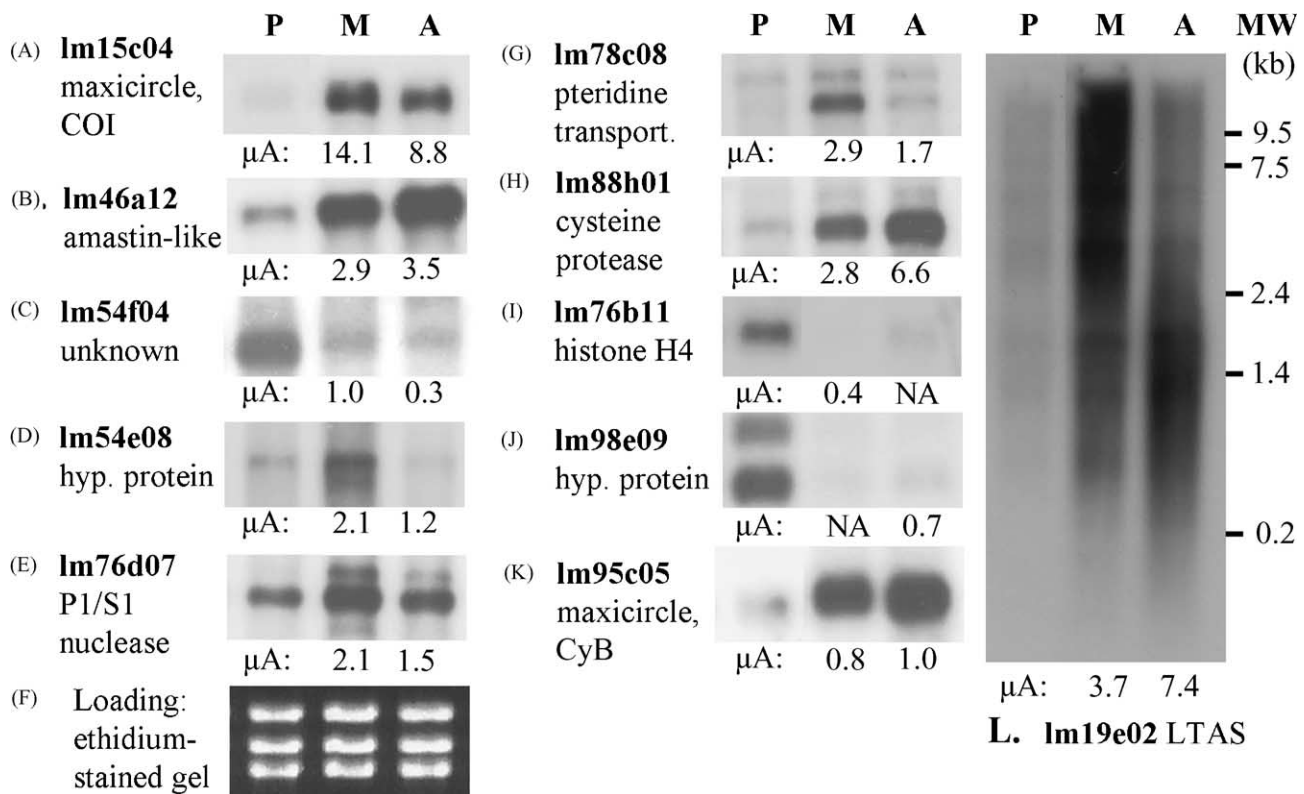

Fig. 3. Northern blot analysis. Panels A–E and G–L: Northern blots were performed with total RNA isolated from logarithmically growing promastigotes (P), metacyclic promastigotes (M), and lesion amastigotes (A), using the indicated hybridization probes. Probe numbers correspond to the genome survey sequence clones reported by Akopyants et al. [17] and the annotations arose from searches of the *Leishmania major* genome project. Only the relevant portion of each blot is shown. The microarray expression ratios (fold-change) of M or A relative to P expression are shown underneath each Northern blot. MW, molecular weight marker. Panel F: A representative ethidium bromide stained gel showing the loading controls of the ribosomal RNAs.

Table 2
Summary and comparisons of Northern blot and microarray data

Spot name	Accession number	Annotation	Band/ smear	Metacyclic/procyclic (log$_2$ ratio)		Amastigotes/procyclic (log$_2$ ratio)	
				Microarray	Northern blot	Microarray	Northern blot
3/3 probes from metacyclic Venn diagram (Fig. 2A)							
lm18c03	AQ846372, AQ848922	Ribosomal region	Bands	−1.26	−1.84	−1.55	−1.60
lm18g10	CC144551, CC144552	Beta-tubulin	Bands	−2.25	−4.32	−2.69	−3.47
lm25g12	AQ845463, AQ845777	Histone H2B	Bands	−3.21	−2.84	−2.21	−1.40
lm35b07	AQ847615, AQ850317	Beta-tubulin	Bands	−1.65	−1.52	−1.76	−1.15
lm94h11	AQ853010, AQ902116	Histone H4	Bands	−2.15	−1.25	−1.25	−1.26
ln10b12	AQ912016	Beta-tubulin	Bands	−2.94	−3.06	−2.69	−2.32
lm52d05	AQ847930, AQ849983	Histone H2A	Bands	−1.97	−1.15	−0.74	−0.45
lm76b11	AZ048291	Histone H4	Bands	−1.42	−4.32	0.00	−1.83
lm02f03	AQ843838, AQ844152	Between *L. major* ORFs	Bands	−1.78	−0.62	−2.00	0.15
lm23h12	BH017650, BH021003	Tuzin	Bands	−2.42	2.40	−1.95	1.60
lm66d08	BH017708, BH017709	ArfGap-like zinc finger protein *L. major*	Bands	−3.63	0.00	−3.15	0.14
lm66f11	BH017714, BH017715	ABC transporter	Bands	−2.36	3.47	−1.59	3.47
lm65c09	BH017688, BH017689	ATP-dependent heat shock protease	Smears	−3.19	0.23	−2.53	−0.76
lm19e02	BH017645, AQ846450	LTAS	Smears	1.89	2.40	2.86	2.06
lm23g06	BH017648, BH017649	Similar to helicase	Smears	1.34	1.15	1.62	0.84
lm31e09	BH021005, BH021006	Maxicircle, COII	Smears	1.58	1.32	1.56	1.03
lm46a12	AQ847712, AQ849643	Amastin 3′ UTR	Bands	1.51	2.56	1.77	1.74
lm88h01	BH017743, BH017744	Cysteine protease	Bands	1.50	1.51	2.72	2.84
lm78d07	BH017728, BH017729, AZ048411	RNA helicase	Bands	1.93	1.56	1.33	0.69
lm16c06	AQ846213, AQ848768	*SHERP*	Bands	1.24	2.32	0.11	0.94
lm24g06	AQ845385, AQ845696	Maxicircle, ND4, G5, ND5	Bands	2.02	0.74	2.12	1.47
lm88h02	BH017745, BH021008	Between two tryp specific ORFs	Bands	1.84	0.14	3.11	0.07
lm66b02	BH017702, BH017703	Between *L. major* ORFs	Smears	1.29	0.62	−0.14	0.71
2/3 probes from metacyclic Venn diagram (Fig. 2A)							
lm09f10	AQ845829	Maxicircle, MURF5, ND7	Bands	1.25	1.32	2.06	2.00
lm20b02	AQ846714, AQ846894	Maxicircle, ND5	Smears	1.24	2.00	1.72	1.40
lm22d04	CC144553, CC144554	Amastin-like	Bands	1.06	2.47	1.38	2.56
lm89h02	BH017748, BH017749	Tryp specific linked to telomere 7	Bands	1.13	1.69	2.19	2.32
lm78c08	AQ853128, AZ048405	Pteridin transporter	Bands	1.47	2.47	0.72	1.12
lm03d07	BH017636, BH017637	P883.16 *L. major*	Bands	1.31	1.47	0.77	0.56
lm15a08	AQ848697	SAM synthetase	Bands	1.07	1.29	0.63	0.42
lm36c09	AQ850729	*SHERP* gene	Bands	1.06	1.64	−0.19	0.18
lm54e08	AQ848018	L4768.01 *L. major*	Bands	1.06	1.29	0.27	−0.06
lm63f03	BH017682, BH017683	*SHERP* gene	Bands	1.60	1.40	−0.31	0.75
lm76d07	BH017726, BH017727, AQ852734	Single strand nuclease	Bands	1.05	1.36	0.52	0.71
ln09f07	No sequence could be obtained		Bands	0.90	4.64	0.17	1.03
lm87h02	BH017742, AQ911606	GlcN:fruc-6-P amidotransferase 2	Bands	1.10	0.56	1.94	−0.38
lm66h04	BH017718, BH017719	*L. major* ORF	*Smears*	*2.02(DS)*	1.32	*3.34(DS)*	0.20
1/3 probes from metacyclic Venn diagram (Fig. 2A)							
lm54f04	BH017668, BH017669, AQ848020	Between *L. major* ORFs	Bands	−0.28	−1.36	−1.68	−1.06
lm21c08	AQ846971	LTAS	Smears	0.83	1.12	1.07	0.84
lm50b02	AQ849525, AQ849823	Tuzin	Bands	0.98	1.29	1.68	1.60
lm76e03	CC144557, CC144558	Amastin-like/tuzin	Bands	0.89	2.94	0.67	2.00
lm14e10	BH017643, BH017644	*myo*-Inositol phosphate synthase	Bands	0.73	0.64	1.35	1.18
lm22e02	AQ846506, AQ846795	NH	Bands	0.86	0.84	1.61	0.23
lm98c05	BH017764, BH017765	Maxicircle, CyB	Bands	1.55	1.64	0.00	2.18

Table 2 (*Continued*)

Spot name	Accession number	Annotation	Band/ smear	Metacyclic/procyclic (log$_2$ ratio)		Amastigotes/procyclic (log$_2$ ratio)	
				Microarray	Northern blot	Microarray	Northern blot
0/3 probes from metacyclic Venn diagram (Fig. 2A)							
lm89h04	BH017752, BH017753	DNA mismatch repair protein	Smears	0.76	0.60	1.23	−0.04
lm20f10	AQ846731, AQ846929	Tryp specific	Smears	−0.77	0.43	−1.13	0.84
lm27a12	AQ850455	Methionine synthase	Bands	0.21	0.76	1.03	1.25
lm10g11	AQ848564	Pteridine transporter	Bands	−0.16	−0.32	−0.13	−0.52
lm12h09	AQ848650	DHFR-TS	Bands	−0.27	−0.14	−0.23	−0.32
lm23d04	AQ846849	gp46	Bands	0.30	0.27	0.14	0.60
lm28d06	CC144545, CC144546	rRNA	Bands	0.16	−0.14	0.07	0.00
lm29e09	AQ847179, AQ851357	NH	Bands	0.06	0.92	0.11	0.94
lm36b02	BH017658, BH017659	NH	Bands	0.34	0.60	0.59	0.56
lm36d09	AQ850737	NH	Bands	−0.31	−0.74	−0.05	−0.89
lm41e05	AQ850678	Alpha tubulin	Bands	−0.54	−0.99	−0.53	−0.74
lm42f06	AQ850865	htf9c	Bands	0.43	0.14	0.22	0.00
lm43f04	AQ849201, AQ851025	Actin	Bands	0.15	−0.52	−0.12	0.00
lm45f04	AQ849062	NH	Bands	0.45	0.00	0.42	0.00
lm47b02	AQ849378, AQ902239	NH	Bands	−0.16	−0.32	0.11	−0.32
lm54g07	AQ848024	Paraflagellar rod	Smears	−0.14	0.90	−0.15	0.64
lm58b07	AQ848177, AQ851892	NH	Smears	−0.05	0.38	0.01	0.38
lm68d08	BH017720, BH017721, AQ852341	*S. cerevisiae* ORF YER129w PAK1;DNA pol α suppressing kinase	Smears	0.02	0.60	0.13	0.06
ln03c02	AQ911379, AQ911822	NH	Bands	0.15	0.67	−0.04	0.00
lm22a06	AQ846486, AQ846766	GNEF guanine nucleotide-exchange protein	Bands	0.73	1.00	1.32	0.30
lm24g05	AQ845384, AQ845695	LTAS	Smears	0.39	1.00	1.36	1.00
lm03g12	CC144549, CC144550	LTAS	Smears	0.76	2.32	0.99	1.56
lm41c06	AQ849106, AQ850660	*myo*-Inositol-1-phosphate synthase	Bands	0.59	1.15	1.02	1.47
lm66g08	BH017716, BH017717	Maxicircle, 9S RNA	Smears	−0.54	1.74	−0.53	1.18
lm68e12	BH017722, BH017723, AQ852351	Arsenite-translocate ATPase	Bands	0.41	1.89	0.34	−0.25
lm85d01	BH017740, BH017741, AQ902392	P100/11E 3′	Bands	−0.37	3.32	−0.29	0.97
lm93b10	AQ852886	Amastin	Bands	0.01	2.25	−0.16	2.32
lm98g04	BH017766, BH017767	NH	Bands	0.24	−1.89	−0.58	−0.25
lm98e09	AQ902641, AQ911728	Hypothetical protein	Bands	0.00	−5.64	−0.49	−2.32

NH: no homology evident in databases. Comparisons shown in gray are ones where Northern blot and microarray were in agreement by the two-fold cut-off. The microarray results are the average of all three replicates; for Venn classifications of less than 3/3, this may account for apparent inconsistencies. Hybridization was not obtained with the following 22 clones: lm65d09, lm65f12, lm22h12, lm66c08, lm65h04, lm08a12, lm66c12, lm63h12, lm81c07, lm88b10, lm61b05, lm22g09, lm32h06, lm29f06, lm09f07, lm22b08, lm44a07, lm55f11, lm68c09, lm68g05, ln02f11, and lm01e04 [17]. DS: a significant microarray dye-swap effect was seen; these were excluded from calculations. Northern blot data for 12 additional maxicircle probes can be found in Table 4. For annotation refer to the Table 3 legend.

The percent confirmation values compared well with those obtained by other workers [32,33]. It should also be noted that the disagreement between the Northern blot and microarray estimates was often minor, reflecting the strict use of the two-fold cutoff.

Secondly, we considered those comparisons in which changes in expression of less than two-fold had been predicted by microarray analysis (i.e., 'not regulated'). For metacyclic versus logarithmic promastigote comparisons, Northern blot analysis confirmed the lack of regulation for 21/36 (58%), while for amastigote versus logarithmic promastigote comparisons this value was 29/37 (78%; Table 2,

Fig. 2). When extrapolated to the numbers of genes classified as 0/3 or 1/3 in the Venn analysis, these data suggest that the microarray experiments failed to identify a significant number of transcripts showing changes in developmental expression.

A supporting perspective comes from 'efficiency' tests; these calculations were based upon genes that were represented multiple times on each microarray, as independent shotgun fragments or specifically designed PCR products. While the inserts differed somewhat in size and 'coverage' of target ORFs, this provided a real-world test of the variability likely to occur for those genes occurring only a single time

in our microarrays. These data showed that the 'efficiency' varied widely for a given locus, ranging from 24–76% of the spots showing two-fold or greater changes in expression. It is likely that a similar fraction was missed in the global analysis. A final perspective comes from comparisons with another study employing our shotgun DNA library collection in expression profiling [34]; remarkably, the overlap in the set of genes identified there for the procyclic– stationary phase transition, with those identified in our study involving metacyclics, was quite low. This will be addressed in the discussion.

3.4. Expression patterns and regulated genes identified

While shotgun DNA library expression profiling failed to identify a large fraction of Northern-blot regulated genes, those that were identified by microarray analysis were subsequently confirmed with good efficiency in Northern blot analysis (68%). In the discussion below we focus on those genes showing regulation in 2/3 or 3/3 microarray experiments per developmental transition, or those confirmed by Northern blot analysis. We determined (and deposited in GenBank) the end-sequences of all of these for which data were not previously available (except for 13 clones where sequence information was not determined due to failure in two or more attempts). When possible we used the then-emerging *L. major* genome sequence to identify the likely gene/ORFs associated with each shotgun

DNA used on the microarrays. For these DNAs, expression ratios ranged from 10-fold down (β-tubulin, histone H2B) to 16-fold up (maxicircle transcripts) relative to procyclics, although most developmental changes were smaller (Tables 2–4). Since our studies focused on three major developmental stages, we adopted a simple approach to clustering and assigned each gene to one of nine possible expression profile 'patterns' (Fig. 4). These classifications must be taken cautiously, due to the significant problem of underestimation noted above.

A number of genes showed procyclic, metacyclic or amastigote-specific changes in transcript abundance. These included genes that were previously identified as stage-specific including up regulation of *HASP* and *SHERP* in metacyclics [35], or histones [36,37] and β-tubulin [38] whose transcripts were more abundant in rapidly dividing procyclic promastigotes, and amastin/tuzin family genes and homologs with expression elevated in amastigotes [12]. We did not identify any transcripts that were elevated in metacyclics/decreased in amastigotes, or the reverse.

The two predominant profiles were those where metacyclic and amastigote transcripts had the same pattern relative to procyclics, either both up or down (Fig. 4; Table 2). This was consistent with the view that metacyclic promastigotes are a pre-adaptive stage, primed for differentiation into the amastigote stage [5]. These genes included ones that were jointly elevated (most maxicircle genes, amastin or tuzin family members, helicase, etc.) or
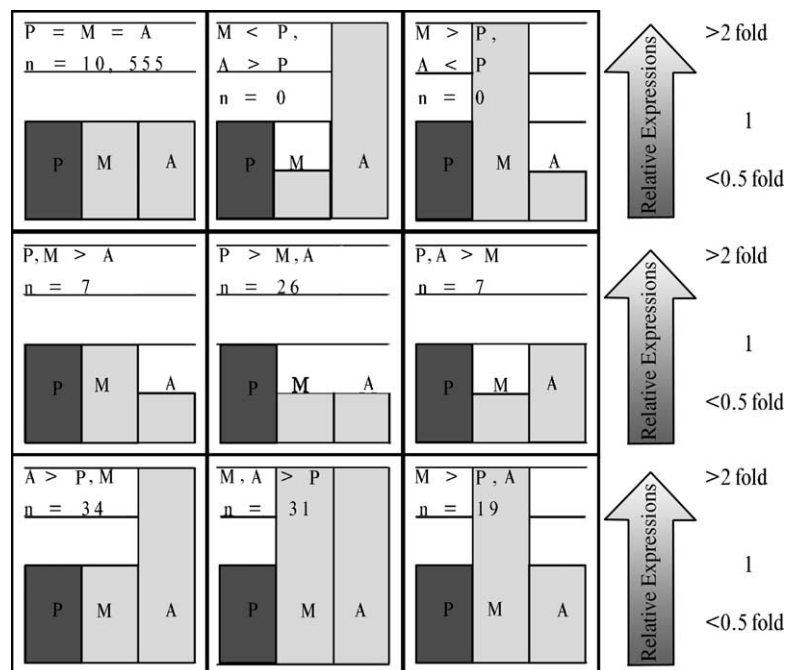

Fig. 4. Expression profiles. For each gene from the 10,464 random shotgun data set, expression in metacyclics or amastigotes relative to amastigotes was scored, using a two-fold cut-off and occurrence in at least 2/3 of the experimental comparisons (Table 1, Fig. 2). For the entire genome, nine potential relative expression profiles are possible, and the total number of genes assigned to each profile is shown in each box. The Y-axis corresponds to expression at least two-fold greater, equal or at least two-fold less than procyclic promastigotes. The X-axis shows the results for comparisons of promastigotes (to facilitate visualization), metacyclic promastigotes (M) or amastigotes (A).

Table 3
Summary of genes assigned to expression profiles showing stage variation

Probe ID	Profile and corresponding gene annotation	M/P log$_2$	A/P log$_2$
P, M > A			
lm01e04	Tryp specific (I)	−0.96	−1.39
lm04c06	No sequence could be obtained	0.28	−1.08
lm20f10	Tryp specific (I)	−0.77	−1.13
lm34e09	No sequence could be obtained	−0.83	−0.93
lm46d01	Multiple hits to single contig, Lm specific (I)	−0.59	−1.10
lm54f04	Between Lm specific ORF and Seq 2 from patent US 6426193: Compounds and methods for detection and prevention *T. cruzi* infection tryp spec (I)	−0.28	−1.68
lm79f02	Cell wall anchor *S. pneumoniae* TIGR4, liver stage antigen, putative *P. falciparum* 3D7, cag pathogenicity island protein *H. pylori* (I)	−1.46	−1.54
P > M, A			
lm01d04	LMBT1 *L. major* mRNA for β-tubulin (D)	−2.92	−2.74
lm01f04	No sequence could be obtained	−1.10	−1.18
lm02f03	Between Lm spec ORF and putative hydrolase of the HAD superfamily *S. typhimurium* LT2 AAL22806.1 (I)	−1.78	−2.00
lm04f07	Between Lm specific ORFs hexamer predictions (I)	−1.07	−1.12
lm05f07	LMBT1 *L. major* mRNA for β-tubulin (D)	−1.69	−1.92
lm18c03	*L. hoogstraali* LSU 24S β ribosomal RNA, *L. donovani* 28S β ribosomal RNA gene, 28S ribosomal RNA subunits δ, ξ, ε (D, I)	−1.26	−1.55
lm18g10	LMBT1 *L. major* mRNA for β-tubulin (D)	−2.25	−2.69
lm22h12	Lm specific hexamer predictions (I)	−1.18	−1.12
lm23h12	Tryp specific tuzin (D)	−2.42	−1.95
lm25g12	AF099108 *L. major* histone H2B variant 1 (D)	−3.21	−2.21
lm34d04	Lm specific P883.16 *L. major* (I)	−0.94	−1.18
lm35b07	L2969.01*L. major*RIKEN cDNA similar to TPR domain containing STI2 *H. sapiens* (I)	−1.65	−1.76
lm36b08	LMBT1 *L. major* β-tubulin (D)	−3.15	−3.25
lm65c09	Regulatory subunit of the HslVU complex ATP-dependent heat shock protease *T. brucei* (I)	−3.19	−2.53
lm65d09	*H. sapiens* cDNA FLJ13633 fis, weakly similar to probable ATP-dependent RNA helicase HAS1 (I)	−2.95	−2.81
lm65f12	Between Lm specific ORFs hexamer predictions (I)	−2.77	−1.72
lm66c08	Between ORFs: similar to TR:O57580 high molecular mass nuclear antigen/*C. fasciculata* RNase H (I)	−2.77	−2.85
lm66d08	ArfGap-like zinc finger protein *L. major* (I)	−3.63	−3.15
lm66e08	Possible monocarboxylate transporter protein *L. major* (I)	−3.82	−2.88
lm66f11	AF200948_1 ABC1 transporter *L. tropica* (D), score improved with (I)	−2.36	−1.59
lm68d08	*S. cerevisiae* ORF YER129w PAK1; DNA pol α suppressing kinase (I)	−2.58	−2.65
lm68d09	Between Lm specific ORFs hexamer predictions (I)	−2.37	−1.98
lm78f02	LMBT1 *L. major* β-tubulin (D)	−1.14	−1.42
lm85h01	AF099108 *L. major* histone H2B variant 1 (D)	−0.92	−1.20
lm94h11	LIH42HIST *L. infantum* H4 histone (D)	−2.15	−1.25
ln10b12	LMBT1 β-Tubulin *L. major* (D)	−2.94	−2.69
A > P, M			
lm03g12	*L. major* telomere-associated sequence (LTAS) (I)	0.76	0.99
lm10b07	*L. major* telomere-associated sequence (LTAS)	0.67	2.09
lm12a08	BCOP coatomer beta subunit *T. brucei* (D)	0.64	1.12
lm14e10	LME344543 *L. mexicana* INO1 *myo*-inositol-1-phosphate synthase (D)	0.73	1.35
lm16g12	Contig too small to be informative	0.84	1.02
lm19a06	Contig too small to be informative	0.29	0.88
lm21c08	Lm specific, missed by hexamer, flanked by *T. cruzi* hits, telomere of chr 7 (I)	0.83	1.07
lm22a06	AF262215_1 guanine nucleotide-exchange protein GEP2 *O. sativa* (I)	0.73	1.32
lm22e02	Contig too small to be informative	0.86	1.61
lm22g06	Lm specific 5′ ORF is AL161316 *L. major* PAC P223 left similar to TR:O35615 friend of GATA-1 (FOG) (I)	1.04	1.12
lm22g09	Tryp specific, missed by hexamer, weak hit to *T. brucei* 28H13.160 GTP-binding elongation factor Tu putative (I)	0.58	1.42
lm22h04	No sequence could be obtained	0.92	1.13
lm24d07	Maxicircle, ND8, ND9, MURF5	0.32	1.24
lm24g05	*L. major* telomere-associated sequence (LTAS) (D)	0.39	1.36
lm25a04	LMU16999 *L. major* ribosomal protein (L-11) gene (I)	0.77	1.29
lm27a12	Methionine synthase, vitamin-B12 independent isozyme AAC76832.1 (I)	0.21	1.03
lm30g06	No sequence could be obtained	0.33	1.05
lm30h06	Tryp specific L1063.05 *L. major* 25N14.175 Ribosomal RNA processing protein (D)	0.52	1.30
lm32h06	L1063.05 *L. major* 25N14.175 ribosomal RNA processing protein (D)	0.74	1.50
lm41c06	LME344543 *L. mexicana* ino1 gene for *myo*-inositol-1-phosphate synthase (D)	0.59	1.02

Table 3 (*Continued*)

Probe ID	Profile and corresponding gene annotation	M/P log$_2$	A/P log$_2$
lm41g11	*L. major* telomere-associated sequence (LTAS) (D)	0.45	1.45
lm50b02	Tuzin (tryp specific) (I)	0.98	1.68
lm53h02	*L. major* telomere-associated sequence (LTAS) (D)	0.59	1.44
lm54f12	No sequence could be obtained	N/A	1.32
lm56g02	Probable DNA polymerase zeta catalytic component *L. major* (D)	0.75	1.25
lm76e03	Amastin-like/tuzin	0.89	0.67
lm79h08	Maxicircle, MURF5	0.11	1.22
lm80g03	Lm specific (I)	0.87	1.38
lm87h01	Tryp specific L3204.02 *L. major* missed by hexamer (D)	0.49	1.11
lm89h03	Human DNA mismatch repair gene (hPMS2), human ribosomal protein L26 (RPL26) (I)	0.69	1.29
lm89h04	Same as lm89h03	0.76	1.23
lm90h02	Tuzin (I)	0.81	1.29
lm95h05	*L. major* telomere-associated sequence (LTAS) (D)	0.93	1.93
ln10g08	Maxicircle, MURF5	−0.46	0.92
M > P, A			
lm03d07	Tryp specific P883.16 *L. major* (D)	1.31	0.77
lm15a08	*L. infantum* LORIEN, and S-adenosylmethionine synthetase (*met*K) (D)	1.07	0.63
lm16c06	LEIFL11A *L. major* fl1.1 (*SHERP* gene) (D)	1.24	0.11
lm36c09	LMA237587 *L. major* *HASPA1*, *HASPB*, *HASPA2*, *SHERP1* and *SHERP2* genes (D)	1.06	−0.19
lm47g01	Tryp specific (I)	0.99	0.94
lm54e08	L4768.01 *L. major* X87839.1 PFRNACRK3 *P. falciparum* serine/threonine protein kinase (I)	1.06	0.27
lm63f03	AJ237587.1 LMA237587 *L. major* cDNA16 gene family (*HASPA1*, *HASPB*, *HASPA2*, *SHERP1* and *SHERP2* genes) (D)	1.60	−0.31
lm66b01	Between 36E18.195 *T. brucei* variant surface glycoprotein, pseudogene/AF461508_1 farnesyltransferase β subunit *L. major* (I)	1.38	−0.21
lm66b02	Between AF272035_1 Rag C *H. sapiens*, AF323609_1 GTPase-interacting protein 2/putative small GTPase *H. sapiens* (I)	1.29	−0.14
lm68b02	Between *H. sapiens* retinol dehydrogenase/G-protein β *A. thaliana*, *S. cerevisiae* (I)	1.22	−0.22
lm76d07	AY079097.1 *L. major* P1/S1 nuclease (D)	1.05	0.52
lm78c08	AF084473_1 pteridine transporter FT5 *L. donovani* (D)	1.47	0.72
lm86g06	AF195531_1 amastin-like surface protein *L. donovani, L. infantum* (D)	1.14	−0.18
lm88b10	No sequence could be obtained	1.07	0.89
lm91a12	M31136.1 LEIHSP70R *L. major* heat shock 70-related protein (D)	1.00	0.19
lm96d02	Tryp specific (I)	0.98	1.03
lm99d11	Lm specific (I)	1.59	−0.10
ln02e11	No sequence could be obtained	1.77	−0.15
ln09f07	No sequence could be obtained	0.90	0.17
P, A > M			
lm43h09	*L. infantum* H4 histone (D)	−0.86	−0.99
lm52d05	*L. donovani, L. infantum* histone H2A, *L infantum* H2A4, H2A5, H2A6 (D)	−1.97	−0.74
lm65h04	*F. nucleatum* mg1 L-met-α-deamino-γ-mercaptomethane-lyase, methyltransferase HgiDIM (I)	−1.30	−0.47
lm68c09	Lm specific (I)	−2.56	−0.89
lm68e12	Lm specific (I)	−1.58	−1.08
lm76b11	*L. infantum* H4 histone (I)	−1.42	N/A
lm91d09	*L. infantum* H4 histone (D)	−1.41	−0.84
M, A > P			
lm02d01	Maxicircle X02438 *L. tarentolae* maxicircle DNA fragment (D)	2.00	2.91
lm08a12	Lm specific 5′ ORF AF115507 *L. donovani* heat shock protein HSP60 (with hits in tryps) (I)	1.66	1.94
lm09f10	Maxicircle, MURF5, ND7	1.25	2.06
lm19e02	*L. major* telomere-associated sequence LTAS (D)	1.89	2.86
lm19e06	Maxicircle M28690.1 LEIND1PUT *L. major* NADH dehydrogenase subunit 1 (ND1) (D)	2.38	2.62
lm20b02	Maxicircle, NADH-ubiquinone oxidoreductase chain 5 (ND5)	1.24	1.72
lm22d04	Amastin-like 5′ ORF is tuzin tryp specific (I)	1.06	1.38
lm23g06	Similar to helicase homolog *H. sapiens, M. musculus* (I)	1.34	1.62
lm24g06	Maxicircle, NADH-ubiquinone oxidoreductase chain 4, 5 (ND4, ND5)	2.02	2.12
lm30g05	Maxicircle, NADH-ubiquinone oxidoreductase chain 5 (ND5)	1.14	1.89
lm31e09	Maxicircle, *L. tarentolae* kinetoplast mitochondrial cytochrome oxidase (COII)	1.58	1.56
lm45g01	Tuzin, tryp specific (D)	1.19	1.06
lm46a12	Lm specific ORF missed by hexamer (I)	1.51	1.77
lm48b10	Maxicircle, Z22728.1 KPLMDIVRB *L. mexicana* kinetoplast divergent region	1.85	4.38
lm59f09	Maxicircle, MURF1 *L. major* NADH dehydrogenase subunit 1 (ND1)	1.50	1.61
lm63h12	Maxicircle, M92830.1 LEIDRC *L. mexicana* cytochrome b	1.01	1.21

Table 3 (*Continued*)

Probe ID	Profile and corresponding gene annotation	M/P log$_2$	A/P log$_2$
lm65h05	I52484 gene PIG-A protein mouse XP_136136.1, GPI-anchor biosynthesis PIG-A XP_204385.1 (D)	0.99	1.85
lm66c12	AL161168 *L. major* cosmid L6823 t7 similar to TR:Q14886 mucin, possibly tryp specific (D)	2.03	1.06
lm68g05	Lm specific missed by hexamer flanking ORF T00243 sopA protein *E. coli* plasmid pO157 (I)	2.47	2.35
lm77d07	Maxicircle, X01094.1 MITBCOX *T. brucei* mitochondrial gene for cytochrome c oxidase subunits I and II (coxI and coxII) (D)	2.25	1.95
lm78d07	DEAD/DEAH box ATP-dependent RNA helicase *P. falciparum* 3D7 CAD50579.1 (D)	1.93	1.33
lm80d12	Maxicircle, *L. tarentolae* mitochondrial 12S ribosomal RNA gene	1.68	2.25
lm81c07	AF339905S3 *L. major* DNA-directed RNA pol III also this clone has LTAS so cannot be assigned definitively (I)	1.24	1.33
lm87h02	X94753 *C. albicans* GFA1 gene for fructose-6-phosphate amidotransferase (D)	1.10	1.94
lm88h01	Cysteine protease *L. major* (D, I)	1.50	2.72
lm88h02	Between two tryp specific ORFs probable mitochondrial oxaloacetate transport protein/*S. pombe* NP_593169.1 (I)	1.84	3.11
lm88h03	Maxicircle, divergent region	0.93	1.64
lm89h01	No sequence could be obtained	0.92	1.57
lm89h02	Tryp specific linked to telomere 7 but no LTAS (I)	1.13	2.19

The table shows the properties of genes assigned to the profiles shown in Table 4. M/P or A/P shows the log$_2$ of the metacyclic or amastigote to promastigote ratio. The average was calculated from all three replicates, regardless of their Venn classification. Clones showing a significant dye-swap (DS) effect in microarray experiments are not shown. Two kinds of comparisons were noted; in many cases, the available DNA sequence for each clone showed a strong similarity to a known gene by BLASTN or TBLASTX search (10^{-20}); these are considered 'direct' hits (D). When a hit was not obtained, we identified the largest assembled portion of the *Leishmania* genome project matching the sequence and performed database searches using 10 kb of sequence flanking either side; in many cases we could identify a nearby ORF that was likely to be the transcript seen by the probe; these are labeled 'indirect' (I). In some cases we were unsure which flanking ORF was identified, and both are then reported. In addition to publicly available sequence, we also searched private collections of sequence for *T. brucei* and *T. cruzi* to discern "tryp specific" GSS, i.e., with similarity hits in other trypanosomes, versus "Lm specific" GSS, having no similarity to any other available sequence. "No sequence could be obtained" indicates GSS that we were unable to obtain sequence despite multiple attempts. "Contig too small" indicates a GSS for which we could not identify a sufficiently large portion of the assembled *Leishmania* genome to perform meaningful similarity searches of the surrounding region. Preliminary sequence data was made available from the *Leishmania* and trypanosome genome sequencing centers (Seattle Biomedical Research Institute, The Institute for Genome Research and Sanger).

decreased (β-tubulin, histones H2B, H4, etc.) in the two stages.

While we did not specifically attempt to study maxicircle gene expression, those occurring in our DNA shotgun library gave good coverage of the majority of known maxicircle genes. Notably, most transcripts arising from the *Leishmania* maxicircle were elevated in both amastigotes and metacyclics. Table 4 summarizes the results obtained from both DNA shotgun microarray expression profiling as well as Northern blot analysis, and comparisons with *T. brucei* are shown in Fig. 5. The agreement between both approaches was good, with a similar 2–4-fold increase in metacyclic and lesion amastigote expression seen for all genes. Two factors need to be considered: first, while many DNA probes identified single maxicircle genes, others spanned two or more (Table 4). However, the overall trend and the presence in some cases of overlapping probes identifying different gene sets suggest that this is not likely to alter the conclusion of up-regulation. Secondly, the potential effect of RNA editing must be considered, as our probes were unedited genomic DNA [39]. Based upon the *L. tarentolae* sequence, the ability of transcripts arising from *MURF5*, *ND7*, *COIII*, *CytB*, *ND1*, *MURF1*, *ND3*, *COII*, *MURF2*, *CO1*, *ND4*, and *ND5* to hybridize to genomic DNA would be expected to be high and unaffected by editing, while for the other probes at least 35% of each gene was potentially able to hybridize to the 1 kb shotgun DNA probes used in microarrays, or Northern blots (Table 4). The effect of editing may account for the

Map	Gene Name	*L. major*	*T. brucei*
	12S rRNA	**M, A > P**	
	9S rRNA		
	ND8	**M, A > P**	**BS > P**
	ND9	**M, A > P**	**BS > P**
	MURF5	**M, A > P**	**BS > P**
	ND7	**M, A > P**	
	CO3		
	CytB	**M, A > P**	**P > BS**
	A6	**M, A > P**	
	MURF1	**M, A > P**	**BS > P**
	G3	**M, A > P**	
	ND1	**M, A > P**	
	CO2	**M, A > P**	**P > BS**
	MURF2	**M, A > P**	**P > BS**
	CO1	**M, A > P**	**P > BS**
	G4	**M, A > P**	
	ND4	**M, A > P**	
	G5 (ND3)	**M, A > P**	
	RPS12	**M, A > P**	
	ND5	**M, A > P**	**BS > P**

Fig. 5. Comparison of maxicircle gene expression in *Leishmania major* and *Trypanosoma brucei*. This figure summarizes the results obtained in the Northern blot and microarray studies found in this work for *Leishmania major*, and Northern blot results previously reported in *Trypanosoma brucei* [54,55]. Missing entries mean that no data are available. The map is based upon that of *L. tarentolae*; white boxes depict genes, within which black regions correspond to extensively edited regions in this species [39]. The abbreviations represent developmental stages; for *Leishmania* these correspond to procyclic promastigote (P), metacyclic promastigote (M) and lesion amastigotes (A), while for trypanosomes this corresponds to culture procyclic (P) and bloodstream (BS) forms. Please see the website maintained by L. Simpson for more details about the trypanosome and *Leishmania* maxicircle and its transcripts (http://dna.kdna.ucla.edu/trypanosome/database.html).

Table 4
Relative developmental expression of *Leishmania major* maxicircle genes

Probe	Genes identified by probe[a]	DNA microarray[b]	Northern blot[c]	Percent probe not affected by editing
lm80d12	*12S rRNA*	*1.7/2.2 (DS)*	*2.1/2.1*	100
lm66g08	*9S rRNA*	−0.5/NA	*1.7/1.2*	100
lm29f06	9S rRNA	−0.2/0.9	No bands	100
lm66g08	ND8	−0.5/NA	*1.7/1.2*	50
lm29f06	ND8, ND9	−0.2/0.9	No bands	50, 35
lm24d07	ND8, ND9, MURF5	*1.0/1.2*	ND	50, 35, 100
lm09f10	*MURF5, ND7*	*1.2/2.1*	*1.3/2.0*	100, 88
lm63h12	*CytB*	*1.0/1.2*	No bands	100
lm98c05	*CytB*	*NA*	*1.6/2.2*	100
lm19e06	*MURF1, G3, ND1*	*1.5/1.6*	*1.4/1.6*	100, 55, 100
lm59f09	*MURF1, G3, ND1*	*2.0/2.6 (DS)*	*1.6/2.2*	100, 55, 100
lm54g04	*ND1, COII*	*2.7/2.7 (DS)*	*2.0/2.5*	100, 99
lm31e09	*COII, MURF2*	*1.6/1.6*	*1.3/1.0*	99, 94
lm77d07	*MURF2*	*2.2/2.0*	ND	100
lm15c04	*COI*	*3.8/3.1 (DS)*	*2.8/2.5*	100
ln03e03	*COI*	*2.1/1.7 (DS)*	*1.1/0.7*	100
lm80g05	*COI, G4*	*2.6/1.6 (DS)*	*1.2/1.3*	100, 50
lm44c10	*G4, ND4*	*2.7/3.1 (DS)*	*1.3/1.5*	50, 100
lm24g06	*ND4, ND3, RPS12*	*2.0/2.1*	*0.7/1.5*	100, 45, 30
lm20b02	*ND5*	*1.2/1.7*	*2.0/1.4*	100
lm02c02	*ND5*	*1.6/0.6 (DS)*	*−0.8/1.5*	100
lm09e03	*ND5*	*2.4/2.8 (DS)*	*0.3/0.4*	100
lm30g05	*ND5*	*1.1/1.9*	ND	100
lm48b10	*ND5*	*1.8/4.4*	ND	100
lm02d01	*Divergent region*	*2.0/2.9*	ND	100
lm19g09	*Divergent region*	*2.9/4.2 (DS)*	*1.8/2.6*	100
lm88h03	*Divergent region*	*0.9/1.6*	ND	100
lm29h06	*Divergent region*	*2.6/4.0*	*1.1/1.8*	100
lm32e03	*Divergent region*	*2.6/4.0(DS)*	ND	100

[a] Genes identified by probe (*L. tarentolae* gene nomenclature).

[b] $\log_2$ ratios (average of three microarray experiments) for metacyclic/amastigote stages compared to procyclic stage. DS, these spots showed significant differences in 'dye-swap' experiments and the microarray result may be unreliable. Italicized numbers mark those showing more than two-fold changes.

[c] $\log_2$ ratios for Northern blot comparisons as in footnote B. ND, not done; NA, not available. Please see the website maintained by L. Simpson for more details about the *L. tarentolae* maxicircle and its transcripts (http://dna.kdna.ucla.edu/trypanosome/database.html).

marginal regulation attributed to *ND8/ND9* (Table 4) and the classification of these probes as elevated in amastigotes (lm24d07, lm79h08 and ln10g08; Table 3). Interestingly, the *ND8/ND9/MURF5* probe lm24d07 showed this pattern, while the adjacent probe lm09f10 containing *MURF5* and *ND7* showed elevated expression in both metacyclic and amastigote stages, which may suggest that *MURF5* does undergo coordinate regulation. It is likely that a more comprehensive analysis of both edited and unedited transcripts may clarify the true situation, and reveal additional regulatory changes.

4. Discussion

Here we undertook a global examination of changes in mRNA expression in the three major forms that occur within the infectious cycle of *Leishmania*, using microarrays based upon random 1 kb shotgun DNA fragments. Three conclusions were drawn: (1) that the fraction of genes whose mRNAs show changes in abundance throughout the infectious cycle seemed to be much lower than seen in other organisms;

(2) that this conclusion was a serious underestimate and that many differentially regulated genes may have been missed, and (3) despite the inefficiency in their identification, a number of genes showed significant changes in stage-specific regulation, including a large number of previously uncharacterized genes. The role of these genes in parasite development is now ripe for further study, and new perspectives on well-known genes such as those encoded by the maxicircle were also obtained.

The conclusion that a modest number of transcripts showed up or down regulation was reached following the analysis of replica experiments comparing metacyclic or amastigote versus procyclic mRNA expression, as summarized in Figs. 1 and 2. The data showed that if a criterion of requiring an expression ratio of at least two-fold in at least 2/3 replicas was used, only ~1% of the genes showed changes in expression. While further analysis suggested that other (lower) cut-offs might be considered, we applied this more conservative value in keeping with other studies and also our own assessment of both experimental and biological relevancy (discussed more below). Notably, our conclusion about the fraction of genes showing significant levels of

regulation was not strongly affected by this choice (Fig. 1), and other methods of statistical analysis yielded similar results about the DNAs showing developmental changes in transcript abundance (analysis not shown). Direct analysis of relative transcript abundance by Northern blot analysis strongly supported results above, with confirmation of 68% of the 'regulated' calls (Fig. 3; Table 2).

Our studies may be compared to previous studies employing similar strategies involving random shotgun DNA libraries in trypanosomatids. In *T. brucei* comparisons involving a library of 21,024 2 kb probes against bloodstream and procyclic form parasite RNAs revealed that about 2% showed greater than two-fold differences in expression [18]. Similarly, in *T. cruzi* comparisons involving a library of 4400 DNAs identified 60 (1.4%) whose transcript levels varied during differentiation from trypomastigotes to amastigotes [40]. Saxena et al. [34] recently reported a study of *L. major* employing our shotgun DNA library set, where RNAs were isolated from promastigotes at various times from growing to stationary phase (some percentage of which are metacyclics [5]). These workers assessed regulation using a statistical *Z*-score based test rather than two-fold cut-off criteria as our studies or those cited above, which often led to classification of genes showing changes in regulation of much less than two-fold. They also used stationary phase rather than purified metacyclic promastigotes, making it difficult to compare their data with ours. These authors concluded that 15% of the genes showed statistically significant changes in expression at one or more time point in transition, with 1.3% showing regulation at two or more time points. Remarkably, and in contrast to our results, the methods used there did not yield many classic genes showing up or down regulation in metacyclics in previous studies. Moreover, if one applies the standard two-fold cut-off criterion to their findings, the number of transcripts showing differential expression drops considerably to a range similar to that found in our study.

Another study using 2000 EST probes encompassing ∼1000 genes of *L. major* concluded that about 14% of the genes were significantly up-regulated in lesion-derived amastigotes [41], significantly higher than the 0.6–3.1% found here. As the EST library was not available, we took an *in silico* approach and used EST and shotgun library sequence data to identify 224 DNAs present on our microarrays that are also in the EST library. Of these, we found 9 and 10 scored as regulated in at least 2/3 of our amastigote and metacyclic data sets, respectively (4 and 4.5%), about 3–4 times the level seen in our global analysis. Since the limited EST collection should be skewed towards the most abundant RNAs, potentially this is one contributing factor. As to the remainder, inspection of the data presented by Almeida et al. [41] suggests that in fact the fraction of genes showing significant regulation may be comparable to our upper estimates (3.1%), with Almeida et al. assigning significance to differences that we do not due to the incorporation of clustering methodology. Thus, effectively all four studies using double-stranded DNA probes reached

a similar conclusion about the relative paucity of genes showing differential expression.

Despite the agreement of the findings above with prior studies in trypanosomatids, we challenged our findings by performing a large number of Northern blot comparisons. As noted earlier, about 68% of the genes showing differential expression in shotgun microarray comparisons were confirmed by Northern blots. However, our analysis of genes assigned to the 1/3 and 0/3 Venn microarray classes, and thus considered to be 'unregulated' by these criterion, revealed that 32% of these showed greater than two-fold changes in expression by Northern blot analysis (Fig. 2, Table 1). Since the 0/3 and 1/3 Venn microarray classes represent the vast majority of genes, these and other findings suggest that in fact DNA shotgun library expression profiling greatly underestimates the true fraction of transcripts showing significant changes in expression. Perhaps more tellingly, the set of genes identified in our study showed little overlap with those identified in the procyclic-stationary phase transition in a prior study using our *Leishmania* shotgun DNA library [34]. As in our study, Northern blot analysis confirmed differential regulation of most genes identified by microarray. Thus, the discrepancies seem to revolve around genes whose differential expression was missed, by either microarray study.

Collectively, these studies argue that the use of shotgun DNA microarrays in these parasites provides at best an imperfect perspective on changes in transcript abundance. Why should this be the case in *Leishmania*, in contrast to their success in other organisms? One factor may be that the *Leishmania* genome, while lacking in interspersed repetitive DNA elements, nonetheless contains a variety of simple sequence repeats ranging upwards from the common dinucleotide repeats (CA:GT, CT:GA); these are most prevalent in 'inter-transcript' regions but also occur within mRNAs [42]. Secondly, for a number of genes antisense transcription and transcripts have been identified, which could show differential expression during development [43–46]. Both of these factors would lead to underestimates in assessing changes in relative expression in microarray analysis by effectively increasing 'background' hybridization, and for genes undergoing only modest changes, would lead to their being missed entirely. These notions lead to the prediction that both of these factors would be mitigated if strand-specific, 'coding-region' specific probes were used for microarrays, and some evidence supporting these ideas may be evident in the EST comparisons discussed above [41]. Recently, microarrays using long oligonucleotides with these properties have been developed, and we are currently testing whether these show improved performance by the criteria established above.

Previous surveys seeking to identify stage-regulated transcripts in *Leishmania* have revealed remarkably few [8–12]. However, in general the methods used preferentially yield genes whose transcript abundances differ greatly, to the exclusion in some cases of those showing more modest changes. In contrast, in all of the *Leishmania* microarray

studies completed thus far the fold regulation values are typically modest (seldom more than 2–10 folds). This suggests the interesting possibility that regulation in *Leishmania* primarily involves smaller changes in mRNA abundance, since as parasites these organisms can rely upon their sand fly or mammalian hosts to provide relatively constant and predictable environments. Similar findings have emerged from studies of a number of viral pathogens, which can exert relatively modest global effects on host mRNA synthesis despite radically affecting overall host metabolism [47,48]. Moreover, the importance of post-transcript regulatory mechanisms have been emphasized extensively in both *Leishmania* and trypanosomes (reviewed in [7,46,49]). Notably, adaptations of expression profiling technology have been developed to probe changes in RNA turnover, synthesis and translation. Our findings also emphasize the value of studies focusing on the *Leishmania* proteome, several of which are underway.

4.1. DNA microarrays as a tool for gene discovery

One goal of this study was to identify genes showing regulation in transcript abundance during the parasite infectious cycle, and in this regard we have identified at least two hundred. These included known genes whose role in parasite biology and virulence are understood or under investigation, summarized in Tables 2 and 3. A number of genes showing relationship to proteins of known function were identified, but whose transcript abundance had not been studied previously. One example involves inositol metabolism, as inositol-1-phosphate synthase transcripts were elevated in amastigotes and metacyclics (Tables 2 and 3). The *Leishmania* surface is heavily populated by inositol-containing molecules including glycosylphosphatidylinositol (GPI) anchors and inositol phosphoceramides [50,51]. GPI-anchored molecules have been implicated in parasite virulence, and inositol is essential for viability [51]. Interestingly, five DNAs containing *Leishmania* telomeric repeat sequences [52] showed up-regulation in both metacyclic and amastigote cells, suggesting the possibility of changes in telomere-associated gene expression, as seen previously in *T. brucei* antigenic variation (reviewed by [53]).

One interesting story involved transcripts from the *Leishmania* maxicircle, which is part of the kinetoplast DNA network and is related to the mitochondrial DNA of other organisms [39,54]. In *T. brucei*, some transcripts show up-regulation in the mammalian bloodstream infecting stages, while others are suppressed (Fig. 5; [54,55]). In contrast, in *Leishmania* it appears that all maxicircle transcripts are up-regulated in both metacyclic and amastigote stages (Table 4, Fig. 5). Our analysis suggests that this finding does not arise from the effects of RNA editing, based upon sequence analysis of the maxicircle DNAs and edited transcripts of *L. tarentolae*. (Table 4). Differences in maxicircle transcript abundance may relate to differences in energy metabolism between the bloodstream trypanosomes

and the intra-phagosomal *Leishmania* amastigotes [56], with a heightened demand occurring in the infective *Leishmania* stages. It is interesting that no nuclearly-encoded genes involved directly in oxidative phosphorylation showed differential regulation (Table 3), however these may have been missed for technical reasons discussed earlier.

References

[1] WHO Expert Committee, 1984. The Leishmaniasis. WHO, Geneva.

[2] Desjeux P, Alvar J. Leishmania/HIV co-infections: epidemiology in Europe. Ann Trop Med Parasitol 2003;97(Suppl 1):3–15.

[3] Hyams KC, Riddle J, Trump DH, Graham JT. Endemic infectious diseases and biological warfare during the Gulf War: a decade of analysis and final concerns. Am J Trop Med Hyg 2001;65:664–70.

[4] Gaskin AA, Schantz P, Jackson J, et al. Visceral leishmaniasis in a New York foxhound kennel. J Vet Intern Med 2002;16:34–44.

[5] Sacks DL. Metacyclogenesis in *Leishmania* promastigotes. Exp Parasitol 1989;69:100–3.

[6] Clayton CE. Control of gene expression in trypanosomes. Prog Nucleic Acids Res Mol Biol 1992;43:37–66.

[7] Clayton CE. Life without transcriptional control? From fly to man and back again. EMBO J 2002;21:1881–8.

[8] Coulson RM, Smith DF. Isolation of genes showing increased or unique expression in the infective promastigotes of *Leishmania major*. Mol Biochem Parasitol 1990;40:63–75.

[9] Charest H, Matlashewski G. Developmental gene expression in *Leishmania donovani*: differential cloning and analysis of an amastigote stage-specific gene. Mol Cell Biol 1994;14:2975–84.

[10] Brodin TN, Heath S, Sacks DL. Genes selectively expressed in the infectious (metacyclic) stage of *Leishmania major* promastigotes encode a potential basic-zipper structural motif. Mol Biochem Parasitol 1992;52:241–50.

[11] Pogue GP, Lee NS, Koul S, Dwyer DM, Nakhasi HL. Identification of differentially expressed *Leishmania donovani* genes using arbitrarily primed polymerase chain reactions. Gene 1995;165:31–8.

[12] Wu Y, El Fakhry Y, Sereno D, Tamar S, Papadopoulou B. A new developmentally regulated gene family in *Leishmania* amastigotes encoding a homolog of amastin surface proteins. Mol Biochem Parasitol 2000;110:345–57.

[13] Sacks D, Noben-Trauth N. The immunology of susceptibility and resistance to *Leishmania major* in mice. Nat Immunol 2002;2:845–58.

[14] Myler PJ, Stuart KD. Recent developments from the *Leishmania* genome project. Curr Opin Microbiol 2000;3:412–6.

[15] Butte A. The use and analysis of microarray data. Nat Rev Drug Discovery 2002;1:951–60.

[16] Moreau Y, Aerts S, De Moor B, De Strooper B, Dabrowski M. Comparison and meta-analysis of microarray data: from the bench to the computer desk. Trends Genet 2003;19:570–7.

[17] Akopyants NS, Clifton SW, Martin J, et al. A survey of the *Leishmania major* Friedlin strain V1 genome by shotgun sequencing: a resource for DNA microarrays and expression profiling. Mol Biochem Parasitol 2001;113:337–40.

[18] Diehl S, Diehl F, El-Sayed N, Clayton C, Hoheisel J. Analysis of stage-specific gene expression in the bloodstream and the procyclic form of *Trypanosoma brucei* using a genomic DNA-microarray. Mol Biochem Parasitol 2002;123:115.

[19] Hayward RE, Derisi JL, Alfadhli S, Kaslow DC, Brown PO, Rathod PK, et al. Shotgun DNA microarrays and stage-specific gene expression in *Plasmodium falciparum* malaria. Mol Microbiol 2000;35:6–14.

[20] LeBowitz JH, Smith HQ, Rusche L, Beverley SM. Coupling of poly(A) site selection and *trans*-splicing in *Leishmania*. Genes Dev 1993;7:996–1007.

[21] Myler PJ, Audleman L, deVos T, et al. *Leishmania major* Friedlin chromosome 1 has an unusual distribution of protein-coding genes. Proc Natl Acad Sci USA 1999;96:2902–6.

[22] Kapler GM, Coburn CM, Beverley SM. Stable transfection of the human parasite *Leishmania major* delineates a 30-kilobase region sufficient for extrachromosomal replication and expression. Mol Cell Biol 1990;10:1084–94.

[23] Glaser TA, Wells SJ, Spithill TW, Pettitt JM, Humphris DC, Mukkada AJ. *Leishmania major* and *L. donovani*: a method for rapid purification of amastigotes. Exp Parasitol 1990;71:343–5.

[24] Medina-Acosta E, Cross GA. Rapid isolation of DNA from trypanosomatid protozoa using a simple 'mini-prep' procedure. Mol Biochem Parasitol 1993;59:327–9.

[25] Sambrook J, Fritsch EF, Maniatis T. Molecular cloning: a laboratory manual. Cold Spring Harbor: Cold Spring Harbor Laboratory Press; 1989.

[26] Hegde P, Qi R, Abernathy K, et al. A concise guide to cDNA microarray analysis. Biotechniques 2000;29:548–50.

[27] Worthey EA, Martinez-Calvillo S, Schnaufer A, et al. *Leishmania major* chromosome 3 contains two long convergent polycistronic gene clusters separated by a tRNA gene. Nucleic Acids Res 2003;31:4201–10.

[28] Lyne R, Burns G, Mata J, et al. Whole-genome microarrays of fission yeast: characteristics, accuracy, reproducibility and processing of array data. BMC Genom 2003;4:27.

[29] DeRisi JL, Iyer VR, Brown PO. Exploring the metabolic and genetic control of gene expression on a genomic scale. Science 1997;278:680–6.

[30] Oono Y, Seki M, Nanjo T, et al. Monitoring expression profiles of *Arabidopsis* gene expression during rehydration process after dehydration using ca. 7000 full-length cDNA microarray. Plant J 2003;34:868–87.

[31] Coller HA, Grandori C, Tamayo P, et al. Expression analysis with oligonucleotide microarrays reveals that MYC regulates genes involved in growth, cell cycle, signaling, and adhesion. Proc Natl Acad Sci USA 2000;97:3260–5.

[32] Dong G, Loukinova E, Chen Z, et al. Molecular profiling of transformed and metastatic murine squamous carcinoma cells by differential display and cDNA microarray reveals altered expression of multiple genes related to growth apoptosis angiogenesis and the NF-kappaB signal pathway. Cancer Res 2001;61:4797–808.

[33] Brown AJ, Planta RJ, Restuhadi F, et al. Transcript analysis of 1003 novel yeast genes using high-throughput northern hybridizations. EMBO J 2001;20:3177–86.

[34] Saxena A, Worthey EA, Yan S, Leland A, Stuart KD, Myler PJ. Evaluation of differential gene expression in *Leishmania major* Friedlin procyclics and metacyclics using DNA microarray analysis. Mol Biochem Parasitol 2003;129:103–14.

[35] Knuepfer E, Stierhof YD, McKean PG, Smith DF. Characterization of a differentially expressed protein that shows an unusual localization to intracellular membranes in *Leishmania major*. Biochem J 2001;356:335–44.

[36] Noll TM, Desponds C, Belli SI, Glaser TA, Fasel NJ. Histone H1 expression varies during the *Leishmania major* life cycle. Mol Biochem Parasitol 1997;84:215–27.

[37] Soto M, Quijada L, Alonso C, Requena JM. Molecular cloning and analysis of expression of the *Leishmania infantum* histone H4 genes. Mol Biochem Parasitol 1997;90:439–47.

[38] Coulson RM, Connor V, Chen JC, Ajioka JW. Differential expression of *Leishmania major* beta-tubulin genes during the acquisition of promastigote infectivity. Mol Biochem Parasitol 1996;82:227–36.

[39] Simpson L, Thiemann OH, Savill NJ, Alfonzo JD, Maslov DA. Evolution of RNA editing in trypanosome mitochondria. Proc Natl Acad Sci USA 2000;97:6986–93.

[40] Minning TA, Bua J, Garcia GA, McGraw RA, Tarleton RL. Microarray profiling of gene expression during trypomastigote to amastigote transition in *Trypanosoma cruzi*. Mol Biochem Parasitol 2003;131:55–64.

[41] Almeida R, Norrish A, Levick M, et al. From genomes to vaccines: *Leishmania* as a model. Philos Trans R Soc Lond B Biol Sci 2002;357:5–11.

[42] Wickstead B, Ersfeld K, Gull K. Repetitive elements in genomes of parasitic protozoa. Microbiol Mol Biol Rev 2003;67:360–75.

[43] Belli SI, Monnerat S, Schaff C, et al. Sense and antisense transcripts in the histone H1 (HIS-1) locus of *Leishmania major*. Int J Parasitol 2003;33:965–75.

[44] Dobson DE, Scholtes LD, Valdez KE, et al. Functional identification of galactosyltransferases (SCGs) required for species-specific modifications of the lipophosphoglycan adhesin controlling *Leishmania major*-sand fly interactions. J Biol Chem 2003;278:15523–31.

[45] Kapler GM, Beverley SM. Transcriptional mapping of the amplified region encoding the dihydrofolate reductase-thymidylate synthase of *Leishmania major* reveals a high density of transcripts, including overlapping and antisense RNAs. Mol Cell Biol 1989;9:3959–72.

[46] Beverley SM. Protozomics: trypanosomatid parasite genetics comes of age. Nat Rev Genet 2003;4:11–9.

[47] Cai Y, Liu Y, Yu D, Zhang X. Down-regulation of transcription of the proapoptotic gene BNip3 in cultured astrocytes by murine coronavirus infection. Virology 2003;316:104–15.

[48] Brum LM, Lopez MC, Varela JC, Baker HV, Moyer RW. Microarray analysis of A549 cells infected with rabbitpox virus (RPV): a comparison of wild-type RPV and RPV deleted for the host range gene, SPI-1. Virology 2003;315:322–34.

[49] Campbell DA, Thomas S, Sturm NR. Transcription in kinetoplastid protozoa: why be normal? Microb Infect 2003;5:1231–40.

[50] McConville MJ, Ferguson MA. The structure, biosynthesis and function of glycosylated phosphatidylinositols in the parasitic protozoa and higher eukaryotes. Biochem J 1993;294:305–24.

[51] Ilg T. Generation of *myo*-inositol-auxotrophic *Leishmania mexicana* mutants by targeted replacement of the *myo*-inositol-1-phosphate synthase gene. Mol Biochem Parasitol 2002;120:151–6.

[52] Fu G, Barker DC. Characterisation of *Leishmania* telomeres reveals unusual telomeric repeats and conserved telomere-associated sequence. Nucleic Acids Res 1998;26:2161–7.

[53] Barry JD, McCulloch R. Antigenic variation in trypanosomes: enhanced phenotypic variation in a eukaryotic parasite. Adv Parasitol 2001;49:1–70.

[54] Stuart KD. Regulation of mitochondrial gene expression in *Trypanosoma brucei*. Bioessays 1987;6:178–81.

[55] Feagin JE, Stuart K. Differential expression of mitochondrial genes between life cycle stages of *Trypanosoma brucei*. Proc Natl Acad Sci USA 1985;82:3380–4.

[56] Burchmore RJ, Barrett MP. Life in vacuoles—nutrient acquisition by *Leishmania* amastigotes. Int J Parasitol 2001;31:1311–20.

[57] Chu S, DeRisi J, Eisen M, et al. The transcriptional program of sporulation in budding yeast. Science 1998;282:699–705.